A Review of Isolation Techniques for 5G MIMO Antennas

Parminder Kaur, Shivani Malhotra, and Manish Sharma

Chitkara University, Punjab, India

Abstract — This paper offers an analysis of mutual coupling reduction techniques used in MIMO antennas designed for sub-6 GHz, 28 GHz, and 28/38 GHz dual frequency bands which are allocated to 5G technology. The said techniques take into account size, gain, isolation, and all diversity-related parameters, such as envelope correlation coefficient (ECC), directive gain (DG), and channel capacity loss (CCL). A review of current technologies is presented in the paper too. The isolation techniques are studied in detail and comparisons between the various works are drawn. Finally, the best isolation technique suitable for specific bands, applications and different port numbers is determined.

Keywords — 5G, isolation, MIMO antenna, mutual coupling

1. Introduction

MIMO (multiple-input multiple-output) is a wireless communication technique capable of simultaneous transmission and reception of many signals over a single frequency channel. Such a method boosts data transfer speeds, expands network capacity, and improves signal quality by using numerous antennas at the transmitter and receiver ends alike. The benefits of MIMO technology include the following:

- higher data rates due to simultaneous broadcasting and receiving of multiple data streams,
- better signal quality, as many antennas allow to minimize the effects of multipath fading and signal distortion,
- longer range achieved by decreasing signal degradation caused by buildings and multipath interference. The MIMO technology may increase the range of wireless networks,
- increased network capacity due to ability to serve, simultaneously, a higher number of users and devices.

While the MIMO approach offers highly advanced features, it also suffers from some drawbacks, as it adds complexity to wireless systems by requiring more antennas and by relying on complicated signal processing techniques, making the solution more challenging to design and deploy. It also adds more cost to the system due to the additional hardware and software needed when relying on the MIMO technology.

Last but not least, it is subject to interference or suffers from mutual coupling between MIMO radiating elements, a phenomenon which degrades signal quality and lowers data throughput rates. Interference caused by other wireless devices using the same frequency band is a factor too.

"Mutual coupling" is a term that refers to a phenomenon in which the radiating antennas used in a MIMO array interfere with each other, degrading the performance of the entire system. This interference occurs due to the electromagnetic waves emitted by one antenna and affecting the other aerials in the array. The causes of mutual coupling in MIMO can be attributed to several factors, such as the placement of antennas in the array, the distance between them, the type, and the orientation of the antennas used.

Three types of mutual coupling may be distinguished [1]:

1) Near-field coupling – the type of coupling that occurs between antennas when they are positioned close to each other. It is characterized by strong electromagnetic fields that can cause interference and signal distortion.

2) Surface wave coupling occurs when MIMO antennas are placed on a conductive surface, such as a metallic plate or a ground plane. This type of coupling is characterized by the propagation of surface waves that may deform the signal. A dispersed current is produced on the ground plane while the antenna element is fed at the feed point. Some energy will be distributed and interference will be produced as a result of this current flowing to the surrounding antenna components.

3) Free space coupling occurs when MIMO antennas are located in the free space and are not subject to any interference or distortion caused by external factors. When electromagnetic waves are radiated outward from the excitation element, some of the energy will be linked to the nearby antennas, thus inducing undesired current.

There are several ways to reduce mutual coupling in MIMO systems. Some of them include increasing the distance between adjacent antennas, using aerials with different radiation patterns and impedance characteristics, exploiting polarization diversity, implementing isolation techniques – such as adding absorptive materials or placing a shield between the MIMO antennas – and optimizing the antenna design by deploying aperture coupling or antenna decoupling techniques, as well as by using frequency-selective structures.

Common types of isolation enhancement techniques used in MIMO include the following.

The polarization isolation technique involves using antennas with different polarization orientations to reduce interference. For instance, if one antenna transmits a horizontally polarized wave, the other antenna may transmit a vertically polarized

signal. This helps reduce signal crosstalk and improves the isolation factor.

The spatial isolation approach involves designing a suitable physical layout of the antennas to help reduce interference. For instance, spacing the antennas further apart or using directional antennas may increase the spatial separation between the antennas, thus reducing mutual interference.

The frequency isolation technique relies on antennas that operate in different frequency bands, which helps reduce mutual coupling and also improves isolation. Interference between antennas is highest when they operate at the same frequency, but frequency-isolated antennas can help mitigate this problem.

In the beamforming technique, the transmitted radiation patterns of the antennas are shaped to reduce interference. Beamforming can be used to steer transmissions away from interfering antennas – an approach which can improve the isolation factor.

Due to its specific usage conditions, the antenna switching technique is also capable of helping improve isolation between antennas.

Overall, these isolation enhancement techniques are vital to the performance of MIMO communication systems, as they reduce signal crosstalk and improve the channel's signal-to-noise ratio, thus leading to higher throughput and data rates.

The specific MIMO isolation or decoupling design approaches may be categorized into two groups: external decoupling techniques and internal decoupling techniques [1]. External decoupling approaches are further divided into neutralization lines (NL), triple line, slots, stubs, parasitic decoupling elements (PDE), defective ground structures (DGS), and those using metamaterials, i.e. relying on the insertion of external structures into the patch or the ground to counteract the mutual coupling effect.

Internal decoupling techniques include space diversity and orthogonal polarization or multi-polarization about polarization diversity.

The remaining techniques used in MIMO antennas are described below.

Neutralization line is a metallic slit used to pass the electromagnetic waves between the elements of the antenna to reduce mutual coupling or improve isolation between the elements. It also improves the bandwidth and reduces antenna size. Electromagnetic bandgap (EBG) structures are made of metallic or dielectric materials with periodic arrangements for the transmission of electromagnetic waves. The periodic structures help achieve independent resonance and attain multiple band gaps, hence reducing mutual coupling and providing high efficiency.

Defected ground structure (DGS) is a type of ground plane etched with defects, slots, or slits to improve efficiency, isolation, and achieve a wide bandwidth, while the antenna with a dielectric resonator is characterized by high radiation efficiency, wide impedance bandwidth, high gain, good isolation, small form factor, and low losses.

Metamaterials have special electromagnetic, isotropic, anisotropic, chiral, photonic frequency-selective surface-based, non-linear, and tunable properties. These features offer enhancements in terms of diversity gain, envelope correlation coefficient (ECC), and wide bandwidth.

Complimentary split ring resonators (CSRRs) consist of two concentric rings with slots opposite each other. They are used to enhance isolation and efficiency and improve diversity gain as well as to reduce the size of the antenna.

The remaining methods relied upon to improve performance and isolation include slots and stubs used to achieve impedance matching, wide bandwidth, high efficiency, and higher gain. Additional parasitic elements around the primary antenna elements mitigate the coupling effect.

The self-isolation method does not involve any external decoupling. The antennas are isolated by maintaining a longer distance between them. Such a method is usually used at sub-6 GHz and mmWave bands. The self-isolation characteristic is often combined with different orientation of antenna elements to achieve spatial and polarization diversities.

In MIMO systems, spatial diversity is used to increase the capacity and reliability of wireless communication through the use of multiple antennas. By transmitting independent signals via each of the antennas, a MIMO system can effectively use the available radio spectrum, reduce errors caused by fading, and increase network capacity.

The polarization diversity technique involves using multiple antennas with different polarizations to receive the same signal simultaneously. Thanks to such an approach, a reduction in signal fading and an improvement in overall signal quality may be achieved. The polarization diversity approach is combined with spatial diversity to further improve signal quality and increase the system's capacity in noisy and fading wireless channels.

2. MIMO Antenna Performance Metrics

This section outlines S-parameters and most important diversity metrics for MIMO antennas with their typical acceptable values summarized in Tab. 1 [1], [2].

The envelope correlation coefficient (ECC) represents the relationship between the isolation factor and the number of antenna elements and in perfect circumstances is equal to zero. To determine the ECC between any number of elements, one can use the radiation field pattern and S-parameters as [3]:

$$\varrho_e = \frac{\left| \iint\limits_{4\pi} \left[\overrightarrow{F_1}(\theta,\phi) \times \overrightarrow{F_2^*}(\theta,\phi) \right] d\Omega \right|^2}{\iint\limits_{4\pi} \left| \overrightarrow{F_1}(\theta,\phi) \right|^2 d\Omega \left| \overrightarrow{F_2}(\theta,\phi) \right|^2 d\Omega}, \quad (1)$$

$$ECC_{(m,n)} = \frac{|S_{mm}^* S_{mn} + S_{nm}^* S_{nn}|^2}{\left(1 - |S_{mm}|^2 - |S_{mn}|^2\right)\left(1 - |S_{nm}|^2 - |S_{nn}|^2\right)} \quad (2)$$

Diversity gain (DG) is a parameter which defines the quality and reliability of a MIMO antenna in wireless systems. Hence,

Tab. 1. S parameter-dependent MIMO design metrics.

Parameter	Value
ECC	< 0.5
DG	<10 dB
TARC	< 0 dB
MEG	−3 dB < MEG < −12 dB
CCL	< 0.4 b/s/Hz

DG must be high (approx. 10 dB) within the acceptable frequency band. DG is also S parameter-dependent and can be calculated, for two ports, as:

$$DG = 10\sqrt{1 - ECC^2}\,. \tag{3}$$

The lower the value of ECC, the better the diversity gain. DG can be optimized by selecting an appropriate number of antennas, spacing, polarizations, and beamforming techniques, among other factors [3].

The total active reflection coefficient (TARC) measures reflected power about incident power and should ideally be zero for MIMO antennas. This metric for a 2-port antenna is calculated from S-parameters and expressed in decibels as [4]:

$$TARC = \frac{\sqrt{(S_{11} + S_{12})^2 + (S_{21} + S_{22})^2}}{\sqrt{2}}\,. \tag{4}$$

Channel capacity loss (CCL) is the highest amount of information that may be sent across a communication link with a low channel loss factor. For MIMO systems, a typical CCL value equals 0.4 bits/s/Hz. The formula for CCL using S-parameters for two ports [4] is:

$$C_{loss} = -\log_2(\sigma^D)\,, \tag{5}$$

where:

$$\sigma^D = \begin{bmatrix} \sigma_{11} & \sigma_{12} \\ \sigma_{21} & \sigma_{22} \end{bmatrix}, \tag{6}$$

$$\sigma_{11} = 1 - \left[|S_{11}|^2 + |S_{12}|^2 \right], \tag{7}$$

$$\sigma_{22} = 1 - \left[|S_{22}|^2 + |S_{21}|^2 \right], \tag{8}$$

$$\sigma_{12} = -\left[S_{11}^* S_{12} + S_{21}^* S_{12} \right], \tag{9}$$

$$\sigma_{21} = -\left[S_{22}^* S_{21} + S_{12}^* S_{21} \right]. \tag{10}$$

The mean effective gain (MEG) measure is defined as the average gain of a MIMO antenna array over all possible propagation channels, taking into account the statistical properties of the channel. Higher MEG values indicate better overall signal strength and improved system performance. MEG can be estimated based on the mutual effect between antenna power gain patterns and the statistical properties of incident radio waves through its vertical and horizontal components which depend on the orientation or polarization. MEG can be calculated as [5]:

$$G_e = \int\limits_{0}^{2\pi} \int\limits_{0}^{\pi} \left[\frac{XPR}{1 + XPR}\, G_\theta(\theta, \varphi)\, P_\theta(\theta, \varphi) \right.$$
$$\left. + \frac{1}{1 + XPR}\, G_\varphi(\theta, \varphi)\, P_\varphi(\theta, \varphi) \right] \sin\theta\, d\theta\, d\varphi\,, \tag{11}$$

where XPR is the cross polarization, $G_\theta(\theta, \varphi), P_\theta(\theta, \varphi)$ are θ components of the antenna power gain pattern and θ components of the angular density functions of incoming plane waves, respectively. $G_\varphi(\theta, \varphi), P_\varphi(\theta, \varphi)$, are the φ components of the antenna power gain pattern and φ components of the angular density functions of incoming plane waves, respectively. Also, $G_e = G_\theta(\theta_s, \varphi_s)$, which shows that MEG corresponds to the directive gain of the antenna in the (θ_s, φ_s) direction, when incoming signals are focused in the (θ_s, φ_s) direction.

The dependence of MEG on S-parameters is as follows:

$$MEG_m = 1 - |S_{mm}|^2 - |S_{mn}|^2, \tag{12}$$

$$MEG_n = 1 - |S_{nn}|^2 - |S_{nm}|^2. \tag{13}$$

3. Review of MIMO Antenna Designs

The 5G frequency spectrum may be split into the lower spectrum, covering frequencies below 6 GHz (also known as sub-6 GHz) and the higher spectrum, covering frequencies over 6 GHz. Therefore, the review of the isolation enhancement techniques and the diversity parameters is based on the aforementioned taxonomy.

3.1. Review of Sub-6 GHz Antenna Design Features

For communicating in the sub-6 GHz band, the design presented in paper [6] provides maximum spatial diversity efficiency of more than 68% and a directive gain over 9.94 dB. The MIMO system with two and four elements showcased in paper [7] did not use any decoupling structures. Instead, the orthogonal orientation of elements is used, which provides high isolation for both systems at all operating frequencies with an efficiency of approximately 85% and a directive gain of 10 dB. In [8], the authors proposed a compact two-element antenna operating in the 5.5–9 GHz band for 5G applications, in which the parasitic element approach has been employed for enhancing isolation and the stepwise modification technique was used to improve bandwidth-related parameters.

In article [9], a dual-band antenna array is proposed with its structure consisting of an L-shaped feeding strip and a Z-shaped radiation strip at the initial stage. Such a design was then modified by adding a rectangular strip as a parasitic element to increase the bandwidth and with an L-shaped strip to make it resonate at 3.4 GHz. Further, a rectangular slit is cut on an additional L-shape strip creating a modified Z-shape that covers the 4.9 GHz band.

Tab. 2. Comparative analysis of decoupling techniques for sub-6 GHz MIMO antennas.

Ref.	Size [mm]	No. of elements	Decoupling technique	Isolation [dB]	Gain [dBi]	ECC	CCL
[6]	55×50×28	4	Spatial diversity, rotational diversity, orthogonal diversity	< −26 11 10	6	< 0.10 0.39 0.28	NC
[7]	23.5×26.5×1.6	4	Polarization diversity	< −30.5/18.5	NC	< 0.001	< 0.4
[8]	40×42×1.6	2	Parasitic element, orthogonal element approach	< −20	6.15	NC	NC
[9]	150×75×6.2	4	Parasitic element approach	< −16.5	4.7/5	< 0.01	NC
[10]	14.9×7×0.8	4	Open loop ring resonator	< −15	4.2	< 0.02	NC
[12]	50×50×1.6	4	Slots	< −11	4.1	0.01	NC

A dual-band antenna with an open loop ring resonator as a feeding element and T-shaped radiating elements is described in [10]. It operates in the 3.3–3.84 GHz and 4.61–5.91 GHz bands. The surface current for 3.5 GHz is directed from the right-hand side of the element towards the center of the substrate and the electric field is routed in the outward direction. The opposite phenomenon occurs for 5.5 GHz, making the proposed antenna of the dual-band type.

A multiband eight-port MIMO aerial is presented in paper [11]. It operates in n2, n3, n39, n65-66 and n77-79 bands. The elements achieve self-isolation through the spatial diversity technique. Another high efficiency 4×4 MIMO antenna for the 3.5 GHz band is presented in article [12]. A circular slot is etched on the antenna unit cell with a radius of 129.79° and with its center coinciding with the center of the ground plane. Each unit cell contributes to the formation of a circular disc

Fig. 1. Isolation techniques for sub-6 GHz band.

in the ground plane. The structure not only provides good isolation, but also offers a peak gain of 4.0 dBi in the 3.4–3.8 GHz frequency range.

The isolation techniques which have been described in the literature are summarized in Fig. 1, while Tab. 2 illustrates the parameters of the described antennas using the individual decoupling techniques.

From Tab. 2, one may conclude that the hybrid of spatial and orthogonal polarization offers maximum isolation and gain for 4-port MIMO antennas while maintaining the expected values of all other parameters.

3.2. MIMO Antennas for 28.0 GHz

The 28 GHz MIMO configuration described in [13] consists of three circular rings surrounded by an infinity-shaped shell. The design offers a peak gain of 6.1 dBi and efficiency of 92%. It is also characterized by spatial and pattern-related diversity required for 5G-based communication. Next, the design was extended to a 1×4 array with a power divider providing a peak gain of 23.5 dBi and a wide bandwidth of 23.58–28.32 GHz.

A 4×4 microstrip patch antenna is proposed in [14], where one element comprises three stubs with a radial structure and stubs being tapered at the outer end. The radiating element is also extended to form an array to provide gain enhancement in the 28–38 GHz range. The array achieves 18.65 dBi of maximum gain with a return loss of −12 dB in the 28–38 GHz range.

A flower-shaped MIMO antenna is proposed in paper [15], where the radiating structure consists of five circular patches, placed 45° apart, and connected to a circular hub through rectangular branches. The ground plane is common and trimmed to enhance gain in the operating band. The antenna achieves −17 dB of isolation and 7.8 dBi of gain.

In [16], a MIMO antenna having T-shaped elements arranged in a row with CPW feed is presented. The design commenced with a single element and a ground plane etched with split
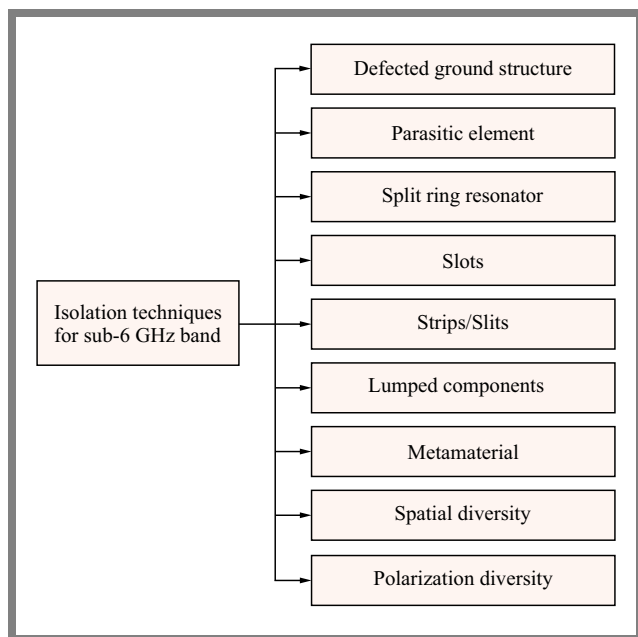
ring slots. Two iterations are then carried out for the etching of split ring slots. A slot in the center with two slots at both of its ends was etched in the partial ground at an optimized distance determined in the first iteration. The second iteration has two even more truncated slots etched in opposite directions at an optimized distance. These slots play a crucial role in the generation of multiple resonant frequencies and provide the bandwidth of 25.1–37.5 GHz, return loss of less than –10 dB, and 10.6 dBi of peak gain at 36 GHz.

In [17], a circular shaped patch has been modified by etching two rectangular slots on either side of the patch to operate in the 28 GHz band, achieving an impedance bandwidth of 26–29.7 GHz. Such a radiating element was next extended to form a four-port MIMO in order to enhance channel capacity. Additionally, DGS was implemented to reduce mutual coupling. A two-element MIMO aerial with isolation of more than 36 dB is presented in [18]. The rectangular-shaped radiators are etched with two slits each and are aligned at 45° in a clockwise direction to achieve high isolation at 29 GHz.

In [19], a dual function DRA-MIMO design is proposed featuring circular polarization in the 25.5–27.79 GHz band. Orthogonal placement of identical ports provides –30 dB of mutual coupling with a gain of 5 dBi and the diversity parameters are within the acceptable limits for 5G communication. An antenna array shown in article [20] provides a low-profile mmWave metamaterial-based MIMO array with two ports, each containing 3×3 unit cells. The antenna achieves high isolation of >24 dB and offers acceptable diversity parameter values over a wide impedance bandwidth with a measured peak gain of 12.4 dBi at 28 GHz.

Authors of work [21] have investigated an antenna with an operational range of 26–29.5 GHz in a 2×2 MIMO configuration, utilizing polarization diversity to obtain a high degree of isolation and a low envelope correlation coefficient.

The MIMO antenna from article [22] has an impedance bandwidth of 9.23 GHz in the 22.43 to 31.66 GHz range and is capable of achieving significant isolation of at least 25 dB between the neighboring MIMO elements, even without the use of decoupling networks. A MIMO antenna consisting of two elements arranged in an array connected through a shared feeding network is proposed in [23]. A bow-tie shaped slot is etched in the middle of the patch with slit on the edges. DGS is deployed by etching vertical and horizontal slots to optimize performance. A zig-zag decoupling structure, as well as spatial and polarization diversity techniques help achieve isolation greater than –40 dB. This antenna operates in the 27.6–28.6 GHz range with its peak gain equaling 12.02 dBi. In Fig. 2, isolation techniques used in the literature for 28 GHz designs are summarized, while Tab. 3 presents a comparison of decoupling techniques with the main parameters of antennas described in recent articles.

From Tab. 3, one may notice that for 2-port MIMO antennas spatial diversity technique brings maximum isolation within the compact size of the antenna, whereas the maximum gain is achieved with designs based on metamaterial or metasurfaces. For 4-port MIMO antennas, the maximum isolation comes from slots, defected ground structures and decouplers, while
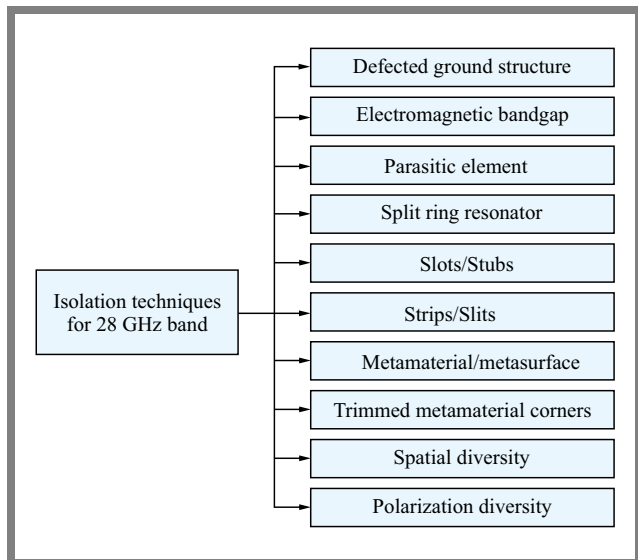

Fig. 2. Review of isolation techniques for MIMO antennas operating in 28.0 GHz band.

gain enhancement is achieved by electromagnetic bandgaps and spatial diversity as well.

3.3. Review of Dual Band Antennas for 28/38 GHz

28 GHz and 38 GHz frequencies are commonly used in 5G dual band antennas due to their low absorption rate.

In article [24], the authors investigated a two-port MIMO antenna with two arrays facing opposite directions. An EBG reflector was installed to minimize backward radiation while simultaneously enhancing the front-to-back ratio. It also helped in achieving a wideband impedance bandwidth with a realized gain of up to 11.5 and 10.9 dBi at 28 and 38 GHz frequencies, respectively.

Article [25] introduces a diamond-shaped pierced patch etched on a defected ground structure for dual-band operation. Orthogonal and spatial diversity techniques are used in four-port MIMO structures to achieve isolation of –50 dB with gain equaling 4.7/3.75 for 28/38 GHz, respectively.

In [26], a four-port MIMO with crescent-shaped radiators is proposed. Partial ground, spatial diversity, and polarization diversity techniques are used to enhance the emitter's isolation from the MIMO structure. The emitter which is 20×20 mm^2 in size exhibits more than –23 dB of isolation and 9.5/11.7 of gain at 28/38 GHz, respectively.

Paper [3] presents the parasitic element approach to two-port MIMO configurations. The isolation measured for the adjacent orientation of elements as well as for face-to-face placement of elements is less than –20 dB over the entire frequency range with a peak gain of 6.6/5.86 dBi at 28/38 GHz, respectively.

The four-port MIMO antenna demonstrated in paper [4] utilizes a parasitic element approach to enhance isolation which improved by 25 dB, with the maximum isolation value equaling –50 dB. The antenna offers a gain of 9.5/11.5 dB for 28/38 GHz bands, respectively. In [27], the authors reported a two port MIMO antenna having rectangular and triangular

Tab. 3. Summary of parameters achieved by decoupling techniques for 28 GHz MIMO antennas.

Ref.	Size [mm]	No. of elements	Decoupling technique	Isolation [dB]	Gain [dBi]	ECC	CCL
[13]	30×30×0.787	4	Pattern diversity	< −29	5.5	< 0.16	–
[14]	30×35×0.254	4	Decoupler and DGS	< −40	–	< 0.01	< 0.4
[15]	25×15×0.787	4	Pattern diversity	< −17	7.8	< 0.0001	–
[16]	12.7×50.8×0.800	4	Spatial diversity	< −22	5	< 0.01	–
[17]	30×30×1.575	4	Slot	< −30	–	< 0.005	< 0.15
[19]	15×30×0.254	2	Spatial diversity	< −35.8	–	< 0.005	< 0.1
[20]	54×23×0.790	2	Metamaterial	< −24	13.4	< 0.0013	< 0.42
[21]	20×20×7.608	4	Pattern diversity	< −25	14.1	< 0.008	–
[22]	24×24×0.254	4	Pattern diversity	< −25	5.6	< 0.0008	–
[23]	30 ×35×0.760	4	Slot	< −40	12	< 0.0003	< 0.4
[29]	110×75×0.760	4	Spatial diversity and DGS	< −22	9.3	< 0.05	< 0.1
[30]	42×85×0.508	2	Metasurface corrugations	< −37.1	18	–	–
[31]	15×25×0.203	2	Pattern diversity	< −30	5.9	< 0.005	< 0.12

stubs added to the radiator along with a partial ground to achieve resonance at 28 and 38 GHz bands. Isolation between MIMO elements is achieved by placing them orthogonally. The reported maximum isolation is less than −20 dB with a peak gain of 5.2/5.3 dBi and isolation of 30/22 for 28/38 GHz, respectively.

A slotted square radiator with a four-port MIMO configuration presented in [28] is characterized by left-hand circular polarization for 28 and 38 GHz bands. For such a design, isolation is below −36 dB and peak gain is 7.03/7.368 dB at 28/38 GHz, respectively.

A slotted rectangular two-port and four-port MIMO is described in article [32], where mutual coupling is reduced to −28.32 dB for the 28 GHz four-port MIMO and −26.27 dB for the 38 GHz four-port MIMO. Gain equals 7.95/8.27 dBi for 28/38 GHz, respectively.

The authors of [33] presented a design of a pentagon-shaped two-port MIMO antenna with a metamaterial array placed between the two symmetrically positioned radiators in order to isolate the electromagnetic fields. The achieved isolation is −39 dB at 28 GHz and −39 dB at 38 GHz with gain equaling 5.2 and 5.5 at 28 and 38 GHz, respectively.

Table 4 summarizes the aforementioned design features and provides the values of specific parameters, while Fig. 3 illustrates isolation techniques used in the literature for dual band antennas.

From Tab. 4, one may observe that metamaterials provide maximum isolation, while hybrid diversity (spatial and polarization) provides maximum gain for 2-port dual-band MIMO antennas, with hybrid diversity ensuring maximum isolation and high gain in 4-port dual-band MIMO antennas.

4. Conclusions

As the number of elements on the same patch increases, the problem of mutual coupling arises and it is a difficult challenge to establish optimum isolation to limit coupling. Numerous techniques have been analyzed which are deployed specifically to reduce mutual coupling or to improve diversity-related parameters. However, increasing gain while maintaining high diversity performance and decreasing the size of MIMO antennas are the few challenges that must be addressed.

This study proves that a substrate with low permittivity and a low loss tangent is necessary for enhancing gain and return loss. In addition, approaches relying on slots, dielectric lenses, and corrugation are required to eliminate the effect of cross-polarization. The use of dielectric lenses and para-
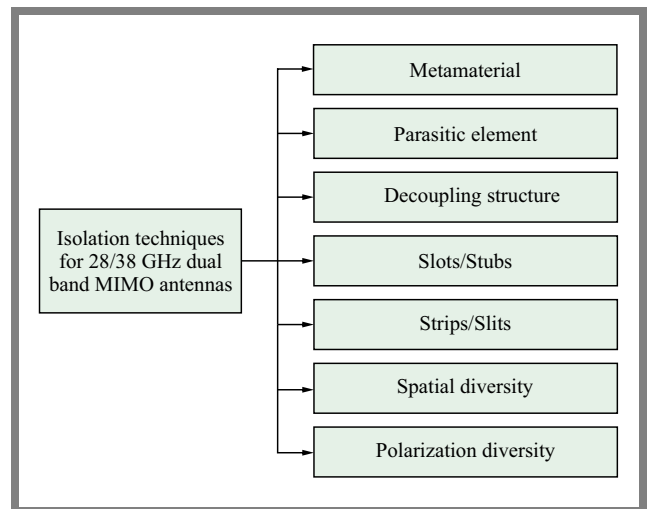
Fig. 3. Isolation techniques for 28/38 GHz band.

Tab. 4. Comparison of parameters of decoupling techniques for 28/38 GHz dual band MIMO antennas.

Ref.	Size [mm]	No. of elements	Decoupling technique	Isolation [dB]	Gain [dBi]	ECC	CCL
[4]	28×28×0.79	4	Parasitic element	−50	9.5/11.5	< 0.001	< 0.01
[24]	20×53×0.203	6	Electromagnetic band gap	< −20	15	< 0.12	−
[25]	150×75×3	4	Polarization and space diversity	−50	4.7/3.75	0	NC
[26]	20×20×0.25	4	Polarization and space diversity	−24/−25	9.5/11.7	< 0.0001	NC
[27]	27.65×12×0.273	2	Polarization and space diversity	−30/−22	5.2/5.3	< 0.0001/ < 0.0002	< 0.4
[28]	100×75×0.508	4	Polarization and space diversity	−36	7.6/8.12	< 0.005	< 0.4
[32]	55×110×0.508	4	Spatial diversity	−28/−26	8.27	< 0.005	NC
[33]	26×14.5×0.508	2	Metamaterial	−39/−38	5.2/5.5	< 0.0001	< 0.05
[34]	27.5×13.5×0.635	2	Spatial diversity	>20/20	NC	< 0.005/ < 0.0002	NC
[35]	30×15×0.203	2	Polarization and space diversity	−32.3/ −36.37	5.7/6.9	$< 10^{-4}$	< 0.3

sitic elements maximizes the radiation in the frontal direction for gain improvement. Metamaterials and DGS improve antenna gain, simultaneously reducing mutual coupling and antenna sizes, while techniques such as dielectric loading, interconnected ground strip, lumped components, orthogonal elements, meta-surfaces, FSS and polarization diversity contribute mostly to isolation improvement.

The major finding of the project is that spatial and polarization diversity isolation techniques (followed by metamaterials and electromagnetic band gap (EBG) techniques) offer higher isolation and improve gain in all the discussed frequency bands for two- and four-port MIMO antennas.

References

[1] K. Du, Y. Wang, and Y. Hu, "Design and Analysis on Decoupling Techniques for MIMO Wireless Systems in 5G Applications", *Applied Sciences*, vol. 12, no. 8, art. no. 3816, 2022 (https://doi.org/10.3390/app12083816).

[2] P. Sharma *et al.*, "MIMO Antennas: Design Approaches, Techniques and Applications", *Sensors*, vol. 22, no. 20, art. no. 7813, 2022 (https://doi.org/10.3390/s22207813).

[3] A.E. Farahat and K.F.A. Hussein, "Dual-band (28/38 GHz) Wideband MIMO Antenna for 5G Mobile Applications", *IEEE Access*, vol. 10, pp. 32213–32223, 2022 (https://doi.org/10.1109/ACCESS.2022.3160724).

[4] M. Hussain *et al.*, "Isolation Improvement of Parasitic Element-loaded Dual-band MIMO Antenna for mmWave Applications", *Micromachines*, vol. 13, no. 11, art. no. 1918, 2022 (https://doi.org/10.3390/mi13111918).

[5] T. Taga, "Analysis for Mean Effective Gain of Mobile Antennas in Land Mobile Radio Environments", *IEEE Transactions on Vehicular Technology*, vol. 39, no. 2, pp. 117–131, 1990 (https://doi.org/10.1109/25.54228).

[6] A. Yacoub, M. Khalifa, and D.N. Aloi, "Compact 2×2 Automotive MIMO Antenna Systems for Sub-6 GHz 5G and V2X Communications", *Progress In Electromagnetics Research B*, vol. 93, pp. 23–46, 2021 (https://doi.org/10.2528/PIERB21031606).

[7] D. Dileepan, S. Natarajan, and R. Rajkumar, "A High Isolation Multiband MIMO Antenna without Decoupling Structure for WLAN/WiMAX/5G Applications", *Progress in Electromagnetics Research C*, vol. 112, pp. 207–219, 2021 (https://doi.org/10.2528/PIERC21032605).

[8] T.M. Guan and S.K.A. Rahim, "Compact Monopole MIMO Antenna for 5G Application", *Microwave and Optical Technology Letters*, vol. 59, no. 5, pp. 1074–1077, 2017 (https://doi.org/10.1002/mop.30475).

[9] J. Huang *et al.*, "A Quad-port Dual-band MIMO Antenna Array for 5G Smartphone Applications", *Electronics*, vol. 10, no. 5, art. no. 542, 2021 (https://doi.org/10.3390/electronics10050542).

[10] J. Huang *et al.*, "Dual-band MIMO Antenna for 5G/WLAN Mobile Terminals", *Micromachines*, vol. 12, no. 5, art. no. 489, 2021 (https://doi.org/10.3390/mi12050489).

[11] Z.F. Al-Azzawi *et al.*, "Designing Eight-port Antenna Array for Multi-band MIMO Applications in 5G Smartphones", *Journal of Telecommunications and Information Technology*, no. 4, 2023 (https://doi.org/10.26636/jtit.2023.4.1297).

[12] S. Saxena *et al.*, "MIMO Antenna with Built-in Circular Shaped Isolator for sub-6 GHz 5G Applications", *Electronics Letters*, vol. 54, no. 8, pp. 478–480, 2018 (https://doi.org/10.1049/el.2017.4514).

[13] M.M. Kamal *et al.*, "Infinity Shell Shaped MIMO Antenna Array for mmWave 5G Applications", *Electronics*, vol. 10, no. 2, art. no. 165, 2021 (https://doi.org/10.3390/electronics10020165).

[14] K.R. Mahmoud and A.M. Montaser, "Optimized 4×4 Millimeter-wave Antenna Array with DGS Using Hybrid ECFO-NM Algorithm for 5G Mobile Networks", *IET Microwaves, Antennas & Propagation*, vol. 11, no. 11, pp. 1516–1523, 2017 (https://doi.org/10.1049/iet-map.2016.0959).

[15] S. Rahman *et al.*, "Nature Inspired MIMO Antenna System for Future mmWave Technologies", *Micromachines*, vol. 11, no. 12, art. no. 1083, 2020 (https://doi.org/10.3390/mi11121083).

[16] S.F. Jilani and A. Alomainy, "Millimeter-wave T-shaped MIMO Antenna with Defected Ground Structures for 5G Cellular Networks", *IET Microwaves, Antennas & Propagation*, vol. 12, no. 5, pp. 672–677, 2018 (https://doi.org/10.1049/iet-map.2017.0467).

[17] M. Hussain *et al.*, "Design and Characterization of Compact Broadband Antenna and its MIMO Configuration for 28 GHz 5G Applications", *Electronics*, vol. 11, no. 4, art. no. 523, 2022 (https://doi.org/10.3390/electronics11040523).

[18] A. Ahmad, D.Y. Choi, and S. Ullah, "A Compact Two Elements MIMO Antenna for 5G Communication", *Scientific Reports*, vol. 12, art. no. 3608, 2022 (https://doi.org/10.1038/s41598-022-07579-5).

[19] A. Kumar *et al.*, "Circularly Polarized Dielectric Resonator Based Two Port Filtenna for Millimeter-wave 5G Communication System", *IETE Technical Review*, vol. 39, no. 6, pp. 1501–1511, 2022 (https://doi.org/10.1080/02564602.2022.2028588).

[20] S.S. Al-Bawri *et al.*, "Hexagonal Shaped Near Zero Index (NZI) Metamaterial Based MIMO Antenna for Millimeter-wave Application", *IEEE Access*, vol. 8, pp. 181003–181013, 2020 (https://doi.org/10.1109/ACCESS.2020.3028377).

[21] N. Hussain, M. Jeong, J. Park, and N. Kim, "A Broadband Circularly Polarized Fabry-Perot Resonant Antenna Using a Single-layered PRS for 5G MIMO Applications", *IEEE Access*, vol. 7, pp. 42897–42907, 2019 (https://doi.org/10.1109/ACCESS.2019.2908441).

[22] M.I. Khan *et al.*, "A Compact mmWave MIMO Antenna for Future Wireless Networks", *Electronics*, vol. 11, no. 15, art. no. 2450, 2022 (https://doi.org/10.3390/electronics11152450).

[23] M. Bilal *et al.*, "High-isolation MIMO Antenna for 5G Millimeter-wave Communication Systems", *Electronics*, vol. 11, no. 6, article no. 962, 2022 (https://doi.org/10.3390/electronics11060962).

[24] A.A.R. Saad and H.A. Mohamed, "Printed Millimeter-wave MIMO-based Slot Antenna Arrays for 5G Networks", *AEU-International Journal of Electronics and Communications*, vol. 99, pp. 59–69, 2019 (https://doi.org/10.1016/j.aeue.2018.11.029).

[25] M.A. El-Hassan, K.F.A. Hussein, and A.E. Farahat, "Compact Dual-band (28/38 GHz) Patch for MIMO Antenna System of Polarization Diversity", *The Applied Computational Electromagnetics Society Journal*, vol. 37, no. 6, pp. 716–725, 2022 (https://doi.org/10.13052/2022.ACES.J.370607).

[26] N. Sghaier *et al.*, "Millimeter-wave Dual-band MIMO Antennas for 5G Wireless Applications", *Journal of Infrared, Millimeter, and Terahertz Waves*, vol. 44, pp. 297–312, 2023 (https://doi.org/10.1007/s10762-023-00914-5).

[27] A.R. Sabek, W.A.E. Ali, and A.A. Ibrahim, "Minimally Coupled Two-element MIMO Antenna with Dual Band (28/38 GHz) for 5G Wireless Communications", *Journal of Infrared, Millimeter, and Terahertz Waves*, vol. 43, pp. 335–348, 2022 (https://doi.org/10.1007/s10762-022-00857-3).

[28] F. Alnemr, M.F. Ahmed, and A.A. Shaalan, "A Compact 28/38 GHz MIMO Circularly Polarized Antenna for 5G Applications", *Journal of Infrared, Millimeter, and Terahertz Waves*, vol. 42, pp. 338–355, 2021 (https://doi.org/10.1007/s10762-021-00770-1).

[29] S.I. Naqvi *et al.*, "Integrated LTE and Millimeter-wave 5G MIMO Antenna System for 4G/5G Wireless Terminals", *Sensors*, vol. 20, no. 14, art. no. 3926, 2020 (https://doi.org/10.3390/s20143926).

[30] S. Gupta, Z. Briqech, A.R. Sebak, and T. Denidni, "Mutual-coupling Reduction Using Metasurface Corrugations for 28 GHz MIMO Applications", *IEEE Antennas and Wireless Propagation Letters*, vol. 16, pp. 2763–2766, 2017 (https://doi.org/10.1109/LAWP.2017.2745050).

[31] H. Zahra *et al.*, "A 28 GHz Broadband Helical Inspired End-fire Antenna and its MIMO Configuration for 5G Pattern Diversity Applications", *Electronics*, vol. 10, no. 4, art. no. 405, 2021 (https://doi.org/10.3390/electronics10040405).

[32] H.M. Marzouk, M.I. Ahmed, and A.A. Shaalan, "Novel Dual-band 28/38 GHz MIMO Antennas for 5G Mobile Applications", *Progress in Electromagnetics Research C*, vol. 93, pp. 103–117, 2019 (https://doi.org/10.2528/PIERC19032303).

[33] B.A. Esmail and S. Koziel, "High Isolation Metamaterial-based Dual-band MIMO Antenna for 5G Millimeter-wave Applications", *AEU-International Journal of Electronics and Communications*, vol. 158, art. no. 154470, 2023 (https://doi.org/10.1016/j.aeue.2022.154470).

[34] A. Omar, M. Hussein, I.J. Rajmohan, and K. Bathich, "Dual-band MIMO Coplanar Waveguide-fed-slot Antenna for 5G Communications", *Heliyon*, vol. 7, no. 4, art. no. 06779, 2021 (https://doi.org/10.1016/j.heliyon.2021.e06779).

[35] W.A.E. Ali, A.A. Ibrahim, and A.E. Ahmed, "Dual-band Millimeter Wave 2×2 MIMO Slot Antenna with Low Mutual Coupling for 5G Networks", *Wireless Personal Communications*, vol. 129, pp. 2959–2976, 2023 (https://doi.org/10.1007/s11277-023-10267-w).

Parminder Kaur, Ph.D.
Chitkara University Institute of Engineering and Technology
https://orcid.org/0000-0001-8161-1505
E-mail: parmindersandal@yahoo.com
Chitkara University, Punjab, India
https://www.chitkara.edu.in

Shivani Malhotra, Ph.D.
Chitkara University Institute of Engineering and Technology
https://orcid.org/0000-0001-8644-4689
E-mail: shivani.malhotra@chitkara.edu.in
Chitkara University, Punjab, India
https://www.chitkara.edu.in

Manish Sharma, Ph.D.
Chitkara University Institute of Engineering and Technology
https://orcid.org/0000-0002-1539-2938
E-mail: manishengineer1978@gmail.com
Chitkara University, Punjab, India
https://www.chitkara.edu.in